MARTIN MARIETTA ENERGY SYSTEMS LIBRARIES

3 4456 0315028 4

ORNL/TM-11159

ornl

OAK RIDGE
NATIONAL
LABORATORY

MARTIN MARIETTA

Crystal Growth and Deformation Behavior of TiAl Aluminides

B. F. Oliver, B. Y. Huang, and
W. C. Oliver

OAK RIDGE NATIONAL LABORATORY
CENTRAL RESEARCH LIBRARY
CIRCULATION SECTION
4500N ROOM 175
LIBRARY LOAN COPY
DO NOT TRANSFER TO ANOTHER PERSON
If you wish someone else to see this
report, send in name with report and
the library will arrange a loan.

OPERATED BY
MARTIN MARIETTA ENERGY SYSTEMS, INC.
FOR THE UNITED STATES
DEPARTMENT OF ENERGY

This report has been reproduced directly from the best available copy.

Available to DOE and DOE contractors from the Office of Scientific and Technical Information, P.O. Box 62, Oak Ridge, TN 37831; prices available from (615) 576-8401, FTS 626-8401.

Available to the public from the National Technical Information Service, U.S. Department of Commerce, 5285 Port Royal Rd., Springfield, VA 22161.
NTIS price codes—Printed Copy: A03 Microfiche A01

This report was prepared as an account of work sponsored by an agency of the United States Government. Neither the United States Government nor any agency thereof, nor any of their employees, makes any warranty, express or implied, or assumes any legal liability or responsibility for the accuracy, completeness, or usefulness of any information, apparatus, product, or process disclosed, or represents that its use would not infringe privately owned rights. Reference herein to any specific commercial product, process, or service by trade name, trademark, manufacturer, or otherwise, does not necessarily constitute or imply its endorsement, recommendation, or favoring by the United States Government or any agency thereof. The views and opinions of authors expressed herein do not necessarily state or reflect those of the United States Government or any agency thereof.

ORNL/TM-11159

Metals and Ceramics Division

CRYSTAL GROWTH AND DEFORMATION BEHAVIOR OF TiAl ALUMINIDES

B. F. Oliver, B. Y. Huang, and
W. C. Oliver

Date Published - April 1990

NOTICE: This document contains information of a preliminary nature. It is subject to revision or correction and therefore does not represent a final report.

Prepared for the
Assistant Secretary for Conservation and Renewable Energy
Office of Energy Utilization Research,
Energy Conversion and Utilization Technologies (ECUT) Division
EG 05 03 00 0

Prepared by the
OAK RIDGE NATIONAL LABORATORY
Oak Ridge, Tennessee 37831-6285
operated by
MARTIN MARIETTA ENERGY SYSTEMS, INC.
for the
U.S. DEPARTMENT OF ENERGY
under contract DE-AC05-84OR21400

MARTIN MARIETTA ENERGY SYSTEMS LIBRARIES

3 4456 0315028 4

CONTENTS

LIST OF FIGURES v

ABSTRACT 1

INTRODUCTION 1

BACKGROUND 2

EXPERIMENTAL APPROACH 4

CRYSTAL GROWTH 4

SLOW GROWTH IN HELIUM 5

RAPID GROWTH IN HELIUM 7

SLOW GROWTH IN HYDROGEN 7

COMPRESSION DEFORMATION 9

ALLOY DEVELOPMENT 14

CONCLUSIONS 22

REFERENCES 23

LIST OF FIGURES

Figure		Page
1	(*a*) Crystal of TiAl grown at 0.023 m/h in helium. Large single-crystal core is evident. (*b*) Laue back reflection results for crystal in (*a*). Pattern "A" is the core crystal, and pattern "a" is for one of the surface grains . .	6
2	(*a*) Laue back reflection results and (*b*) electron diffraction pattern for crystal grown in hydrogen	8
3	$a/2[\bar{1}10]$ dislocations are the first observed after a small amount of deformation	10
4	Tangles of $a/2[\bar{1}10]$ dislocations are observed after a load of 3.11×10^3 N	10
5	$a/2[110]$ and $a/2[\bar{1}10]$ dislocations active after a load of 3.11×10^3 N	11
6	Stereographic projection of TiAl illustrating the change in ϕ during compression	13
7	Stereographic projection of TiAl illustrating the change in θ during compression	14
8	Twin plates formed at a compressive load of 3.56×10^3 N . .	15
9	Diffraction pattern of twins in Fig. 8	15
10	Twins plates formed at a compressive strain of 0.5 and a load of 13.3×10^3 N	16
11	Predominant twin plates of the $(1\bar{1}1)$ type	16
12	Minor twins of the $(\bar{1}\bar{1}1)$ type	17
13	$\langle\bar{1}10\rangle$ dislocations near inclusion	17
14	$(\overline{mn})$, $(\overline{pq})$ dislocations of $a/2[110]$ type	18
15	Hardness as a function of Ti/Al for various ternary alloys	19
16	Wavy slip in TiAl with gallium additions	20
17	Fracture surface of polycrystalline TiAl with gallium additions	21

18 Annealed structure of Ti/Al = 1.0 + 5 at. % Mn. Note annealing twins 21

19 Ti/Al = 1.0 + 5 at. % Mn. 59% compression. Note microtwinning 22

CRYSTAL GROWTH AND DEFORMATION BEHAVIOR OF TiAl ALUMINIDES*

B. F. Oliver,† B. Y. Huang,‡ and
W. C. Oliver

ABSTRACT

This work focuses on the development of single-phase TiAl based alloys. The work has three segments: processing, mechanical testing, and alloying characteristics. The processing consists of developing a technique for growing large, high-purity single crystals. Some of these crystals have been tested to determine their hardness and compression strength. The microstructures of the compressed specimens will be discussed. Finally, two important preliminary findings of the alloy development program concerning additions of gallium and manganese will be discussed.

INTRODUCTION

Titanium aluminides based on TiAl have unique potential for elevated-temperature structural applications. These alloys have low density, high modulus, and good oxidation resistance, and they do not disorder with increasing temperature.[1-4] Such applications include heat engines (i.e., gas turbine engines); however, because of limited room-temperature ductility these alloys are not utilized. Our research is intended to contribute to the understanding of this problem and to identify possible solutions so that more efficient heat engines can be built using TiAl-based alloys.

---

*Research sponsored by the Office of Energy Utilization Research, Energy Conversion and Utilization Technologies (ECUT) Program, U.S. Department of Energy, under contract DE-AC05-84OR21400 with Martin Marietta Energy Systems, Inc. Research performed by the University of Tennessee under subcontract 41B-07685C-S91 with Martin Marietta Energy Systems, Inc.

†Department of Materials Science and Engineering, University of Tennessee, Knoxville, TN.

‡Postdoctoral Fellow, University of Tennessee, Knoxville, TN.

This study focuses on the processing and slip behavior of TiAl alloys. Although significant studies of TiAl alloys are in progress elsewhere, this is the only program focusing on single-crystal, single-phase TiAl alloys. Studying slip in single crystals of TiAl-based alloys can bring new understanding of the causes of their low room-temperature ductilities. The alloy development portion of this study will also focus on single-phase, single-crystal materials. Alloying additions with potential for increasing the ductility of TiAl-based alloys will be identified and the dislocation structures of deformed specimens will be studied so that the effects of these alloying additions on the character, distribution, and density of dislocations can be determined.

BACKGROUND

Mechanical property investigations of the pure compound TiAl, as well as of alloyed single-crystal material, is the objective of this program. The utilization of TiAl-based alloys is limited because of their lack of ambient temperature ductility. Investigations have been carried out to further understand the mechanical behavior of these intermetallics.[5-8] Other research indicates that single-crystal compounds, as well as alloyed single-crystal compounds, can have superior mechanical properties.[9] In order to begin studies of the basic mechanical properties of these aluminides, we undertook an investigation to determine how to grow relatively large single crystals of TiAl.

A system for single-crystal growth employing containerless directional solidification has been developed.[10-14] Induction heating is utilized to both melt a liquid zone and electromagnetically levitate and shape the zone.[15] Stability of the liquid zone shape is not primarily determined by surface tension effects but by the distribution body forces effecting levitation of the liquid zone. This method is crucibleless and permits a wide variety of processing atmospheres for crystal growth. Containerless melting minimizes contamination and provides the ability to grow crystals of intermetallic compounds at slightly positive pressures, facilitating some control of the resulting stoichiometry. Fluid mixing in the liquid zone is nearly turbulent or at least very highly stirred.[11] The growing

solid-liquid interface is rotated so as to enhance mixing. Good-quality single crystals 2.54×10^{-2} m in diam and 10 to 15×10^{-2} m in length of aluminum-rich TiAl have been grown from the near-turbulent melts. Optical microscopy, X-ray Laue back reflection, and transmission electron microscopy (TEM) have been used to evaluate the quality of single crystals grown under different processing conditions. The crystal growth process is computer controlled, utilizing image processing for crystal dimensional control and, where appropriate, infrared sensing for temperature control. The diameter of the growing interface and the grown crystal can be controlled to 76 μm. The system uses a DEC, PDP 11/23 computer with the RT-11 operating system. The control system characteristics will be reported separately.

Fat-Halla et al. reported growing single crystals of TiAl by a floating-zone method.[16,17] While these researchers did not report the details of their method nor the size of the crystals grown, the method was probably dependent upon surface tension for stabilization of the liquid zone. They reported growing single-phase, single-crystalline material from 40.8 to 45.9 at. % titanium. The higher the titanium content, the slower the required growth velocity for single crystals (down to 8.9×10^{-3} m/h) if the crystal was to be without substructure or second phases.

As previously stated, the aluminide TiAl is known to be quite brittle at ambient temperatures. Considerable work has been devoted to understanding the mechanism of this brittle behavior.[3,5-8,18,19] Single-phase polycrystalline TiAl was tested in compression by Lipsitt and co-workers.[7-8] Their material contained more carbon and oxygen and was richer in titanium than the single-crystal material examined here. They observed a/2<110> ordinary dislocations and a<011> superlattice dislocations. The a<011> dislocations generate the a/6<112> type partial dislocations and stacking faults. They considered a/2<110> type dislocations a constituent of the hard slip mode a<011> superdislocations. These results would indicate that the mobility of the superlattice dislocations controls the plasticity of TiAl. In 1985, T. Kawabata et al. tested a single crystal in compression with [010] orientation.[17] They found that the mobility of the a/2<110> dislocations did not differ much from that of the a<011> superlattice dislocations below the peak yield

stress temperature. In 1986 Hug et al. reported a/2<112> type dislocations in TiAl.[20] They considered these a/2<112> superdislocations to be important in the plastic deformation process. In 1987 T. Kawabata found that at temperatures of 77 K the a/2<110> ordinary dislocations were immobile but a<101> and a/2<112> superdislocations contributed to the plastic deformation.[21]

EXPERIMENTAL APPROACH

The overall objective of this study is to identify and understand mechanisms of plastic deformation of TiAl-based alloys. The overall approach consists of three major efforts, as follows. First, large single crystals of TiAl-based alloys must be grown as raw material for mechanical testing. Process parameters that can be varied include the growth atmosphere, growth rate, and starting composition. Second, samples are cut from this material and compressed to various stress levels and the resulting dislocation structures studied. In particular, the active slip systems must be identified. Finally, ternary alloys with improved mechanical properties that stay within the single-phase constraints of this program will be developed. The initial study will focus on the hardness and microstructural changes associated with various alloying additions.

CRYSTAL GROWTH

Arc-melted and drop-cast ingots (44 at. % Ti, 56 at. % Al) 2.5×10^{-2} m in diam by 0.15 m long were used as starting material. These ingots were assembled into a 0.38-m assembly involving reusable end pieces of nickel. Samples were levitation-zone processed (one pass) in one atmosphere of purified helium or ultrapure hydrogen. Although the as-cast (AC) results for ingot 11195 are not available, the AC results for 11588 should be viewed as typical. The results obtained in each atmosphere were distinctly different, hence subsequent processing of this intermetallic compound was performed in the ultrapure hydrogen atmosphere. Table 1 compares the conditions of processing and the resulting chemical analyses for interstitials on two processed ingots. Crystals grown faster than approximately 2.5×10^{-2} m/h exhibit a strong substructure.

Table 1. Melt comparisons

Ingot[a]	dph (2-kg load)	Weight (ppm)				Melt conditions
		C	N	O	H	
11195 AC	–	–	–	–	–	Pure He
ZB	255	100	31	241	–	0.023 m/h
ZE	–	85	36	374	–	100 rpm
11588 AC	–	124	39	605	–	Pure H_2
ZB	269	129	37	104	<1	0.023 m/h
ZE	269	106	30	295	<1	100 rpm

[a]AC, as cast; ZB, zone beginning; ZE, zone end.

Two points should be noted concerning the results shown in Table 1. First, the composition shown in the zone-beginning (ZB) section of the 11588 ingot indicates extremely low interstitial contents. Second, the low hydrogen levels in the ingot grown in hydrogen suggest that these alloys may be very resistant to hydrogen embrittlement.

SLOW GROWTH IN HELIUM

Ingot 11195 of Table 1 was sectioned and metallographically prepared. A transverse macrosection is shown in Fig. 1(*a*). The 2.5×10^{-2}-m-diam section shows a single crystal core surrounded by surface grains. The surface grains run the full processed length of the specimen. The grain boundaries on the freely frozen surface were so straight that they were at first thought to be twins by their surface macro-appearance. Figure 1(*b*) also gives the growth direction of the core crystal, 9° off [011]. The orientations of the surface crystals are only slightly rotated from the core crystal orientation. The results of a selected area Laue back reflection pattern of a 1-mm-diam area containing the core (A) and one of the surface crystals (a) is also shown. The solid lines are several of the zones of the back reflection pattern. The surface crystals are oriented a few degrees off the core crystal. One growth twin was observed on

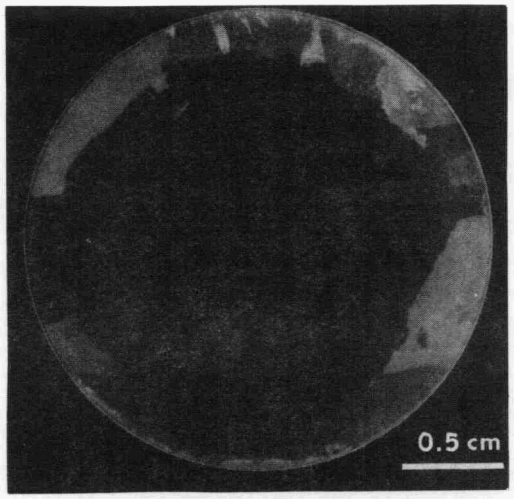

(*a*)

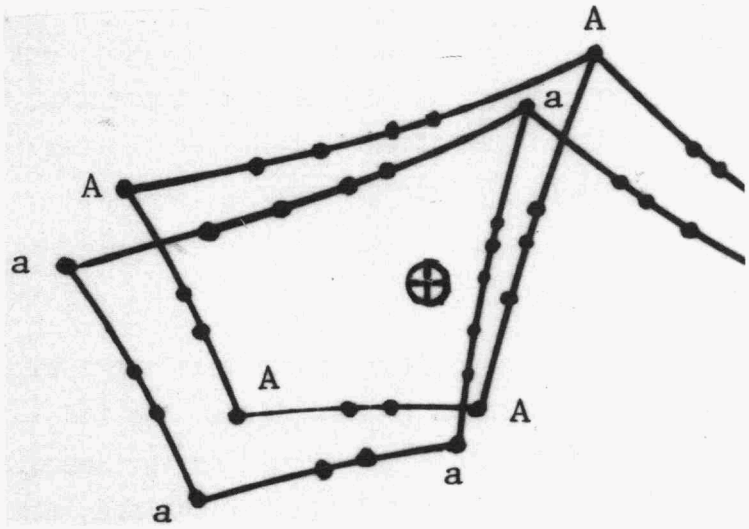

(*b*)

Fig. 1. (*a*) Crystal of TiAl grown at 0.023 m/h in helium. Large single-crystal core is evident. (*b*) Laue back reflection results for crystal in (*a*). Pattern "A" is the core crystal, and pattern "a" is for one of the surface grains. *Source:* University of Tennessee, Knoxville.

this specimen. The (111) and ($\bar{1}\bar{1}2$) mirror planes for this twin were determined by the stereographic projection with the identified poles of the Laue pattern taken from the twin boundary. X-ray phase analysis of both the core and surface crystals show that both are single-phase. No diffraction peaks of phases other than TiAl were observed.

RAPID GROWTH IN HELIUM

Crystal growth in helium at growth velocities greater than 2.54×10^{-2} m/h and 100 rpm of the freezing interface results in a distinct substructure. Laue back reflection results for such a rapidly grown crystal evidence a double spot pattern indicating about 2° of orientation difference. The resulting crystal is single-phase with an occasional small interior grain. A strong anisotropy of crystal growth is evident at all growth velocities.

SLOW GROWTH IN HYDROGEN

The pure hydrogen atmosphere is produced by diffusion through a palladium-silver alloy into the melt chamber. The chamber is then sealed off at slightly more than one atmosphere and continuously gettered with a heated titanium coil.

Ingot 11588 (Table 1) was entirely a single crystal with no surface grains. The best-quality crystals of TiAl were grown in a pure hydrogen atmosphere at 2.2×10^{-2} m/h. Figure 2(*a*) shows the Laue back reflection pattern of this single crystal with the growth direction as 18° off [011]. Metallographic examination also indicated that no substructure was present. All test results to date indicate that the single-crystal growth direction of TiAl is near [011].

The quality of the crystal grown in hydrogen was examined further by preparing samples for TEM examination. Since TiAl is extremely brittle at room temperature, samples were electrical-discharge-machined from the single crystal. Further thinning to 0.24 mm was done by electrolytic polishing, with the current and voltage adjusted for uniform thinning. Final jet polishing with a solution of perchloric acid, ethanol, and butoxye-ethanol at −10°C produced samples suitable for examination.

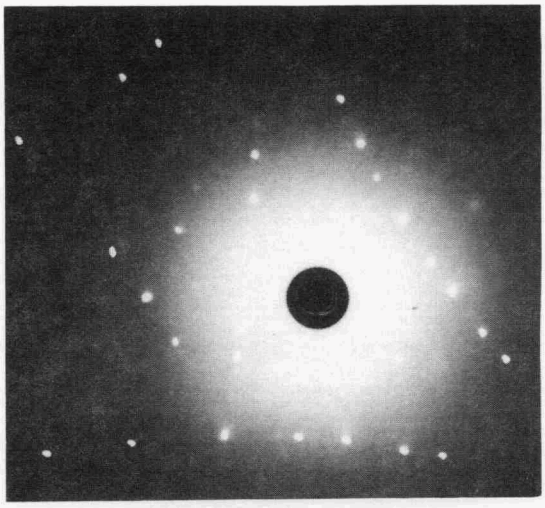

(*a*)

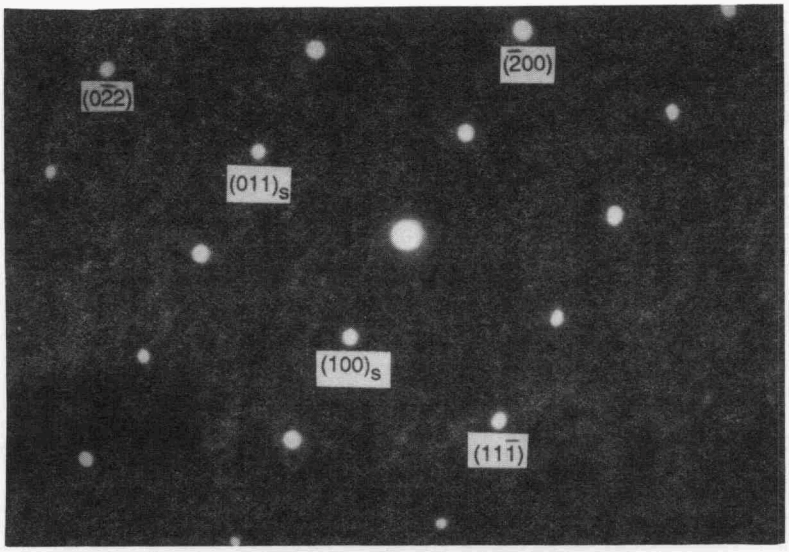

(*b*)

Fig. 2. (*a*) Laue back reflection results and (*b*) electron diffraction pattern for crystal grown in hydrogen. *Source:* University of Tennessee, Knoxville.

Transmission electron microscopy showed a generally clean structure with an occasional fine particle. Diffraction patterns taken anywhere in the samples showed results as in Fig. 2(*b*), where (011)s and (100)s are superlattice diffraction spots.

The crystal designated 11588 was selected for mechanical testing. This crystal composition is on the alunimum-rich side of the g phase field, and no substructure was observed in the as-grown crystal. Annealing portions of the crystal at 1000°C for 7 d did not change the intensity of superlattice Debye diffraction lines. Hence, it was not necessary to heat-treat the crystal before testing. Since the g single crystal is very brittle, 3-mm-diam disk samples for compression testing were electrical-discharge-machined from the large crystal. The disks were compressed at room temperature at different loads (2.2, 2.67, 3.11, 3.56, and 13.34 × 103 N). Thinning the compressed sample to the thickness required for TEM examination was done by electropolishing, followed by final jet polishing with the same solution mentioned above. During operations, these specimens were held in a special platinum foil to avoid brittle fracture.

COMPRESSION DEFORMATION

The first sample was compressed at a load of 2.67×10^3 N. At this compressive load, transmission microscopy indicates that the dislocations are generated and begin to move. Figure 3 shows the generated dislocations and their probable direction of motion. They were identified as $a/2[\bar{1}10]$ ordinary dislocations by using their invisibility criterion for $g = [11\bar{1}]$. It is consistent with the Schmid law that the $a/2[\bar{1}10]$ dislocations were generated and first to move. For the given compressive direction, the (111) $[\bar{1}10]$ slip system has the largest Schmid factor of 0.47. (This is shown in Figs. 7 and 8 and discussed below.)

The sample loaded at 3.11×10^3 N contained low-density $a/2[\bar{1}10]$ dislocation tangles. Figure 4 shows this dislocation configuration. At this stress level some a/2[110] ordinary dislocations were also observed, (Fig. 5) quite near the $a/2[\bar{1}10]$ tangles.

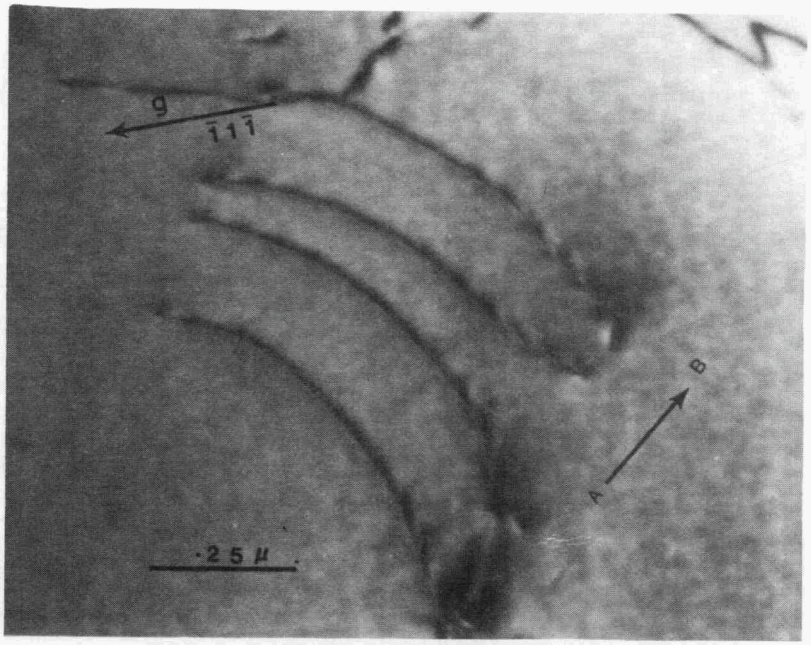

Fig. 3. a/2[$\bar{1}$10] dislocations are the first observed after a small amount of deformation. *Source:* University of Tennessee, Knoxville.

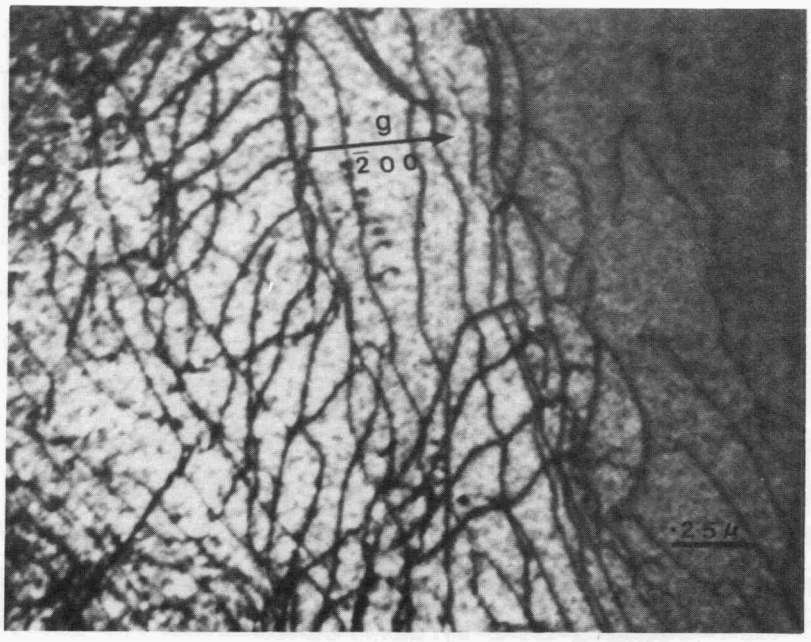

Fig. 4. Tangles of a/2[$\bar{1}$10] dislocations are observed after a load of 3.11×10^3 N. *Source:* University of Tennessee, Knoxville.

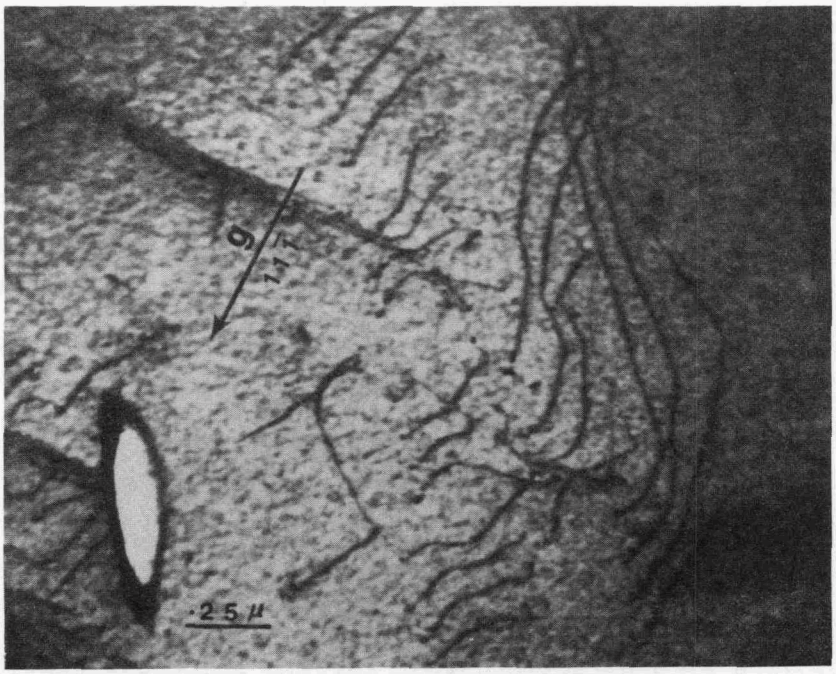

Fig. 5. a/2[110] and a/2[$\bar{1}$10] dislocations active after a load of 3.11 × 10^3 N. *Source:* University of Tennessee, Knoxville.

The a/2[110] dislocations are on a secondary active slip system and are discussed using Figs. 6 and 7. Figure 6 locates the specimen load axis (and growth direction) on the stereographic projection. This growth direction of 18° off [011] and 60° off [$\bar{1}$11] has been previously reported.[22] There are five interesting regions in Fig. 6. Region A is the triangle [$\bar{1}$11]–[010]–[011] containing the primary slip system (111) [$\bar{1}$10]. Region B contains the primary slip system ($\bar{1}$11) [110], triangle C the super dislocation slip system (1$\bar{1}$1) [011], triangle D the super dislocation slip system (111) [101], and triangle E the super dislocation slip system (111) [$\bar{1}$01]. The <110> directions are not equivalent to the <011> directions in this crystal structure. Considering Schmid's law, ϕ is defined as the angle between the normal of the slip plane and the tensile axis, and θ is the angle between the tensile axis and the slip direction. For compression tests the slip system rotation is quite different from that in tension considering the changes in both θ and ϕ. Figure 6 shows the path of rotation of the normal to the slip plane,

relative to the loading axis for the TiAl single crystal, as the load increases through the yield stress.[23-26] The angle between the load axis and the normal to the (111) slip plane is ϕ_0. Slip begins first on the primary slip system (111) [$\bar{1}$10]. If ϕ is considered in this compression test, it decreases from ϕ_0 to ϕ_1 along the path between the load direction and [111]. This describes the rotation of the angle for the primary slip system. ϕ_1 is on the boundary between triangles A and B. At this boundary the secondary slip system ($\bar{1}$11) [110] is activated. The path ϕ_1 – ($\bar{1}$11) describes the angle for this secondary slip system. The [011] pole in Fig. 6 is the point at which the slip systems for triangles D and E could be activated; however, because the burgers vector for <011> slip would be twice as long, a somewhat higher stress will be required. If a/2<011> is used, a complex fault will result. Referring to Fig. 7, analogous arguments apply to $\phi_0 - \theta$.

Two possible slip directions that involve super dislocations are [$\bar{1}$01] and [010]. Experimental dislocation configurations obtained from the TEM work confirms the analysis presented above. Neither the superdislocation <011> nor <010> was observed in any of the samples. Thus, we can limit our study to only the ordinary dislocations in the single-crystal TiAl structure in this orientation.

When the load on the single-crystal specimen is 3.56×10^3 N, twins are observed. The twin plates are shown in Fig. 8. A diffraction pattern from the twin plates is shown in Fig. 9. These twins have a ($\bar{1}1\bar{1}$) axis. Occasional twins appeared at lower compressive loads. Finally, a sample was loaded to 13.3×10^3 N which resulted in a total compressive strain of 0.5. The cracks in this sample after compression run from the top to the bottom of the tested disk, with the sample material still continuous. A very high density of twin plates was observed everywhere in this sample (Fig. 10). A diffraction pattern from these twins is shown in Fig. 11. The minor twin axis in Fig. 10 is ($\bar{1}\bar{1}$1), as identified Fig. 12. The latter occurs less often than the ($\bar{1}1\bar{1}$) twins.

Figure 13 is a micrograph taken from a sample that had a small inclusion. This sample was compressed at a load of 2.2×10^3 N. The inclusion is on the right bottom of Fig. 13 in the dark area and is more clearly shown in Fig. 14. EDAX analysis indicates that this particle has

ORNL-DWG 88-14101

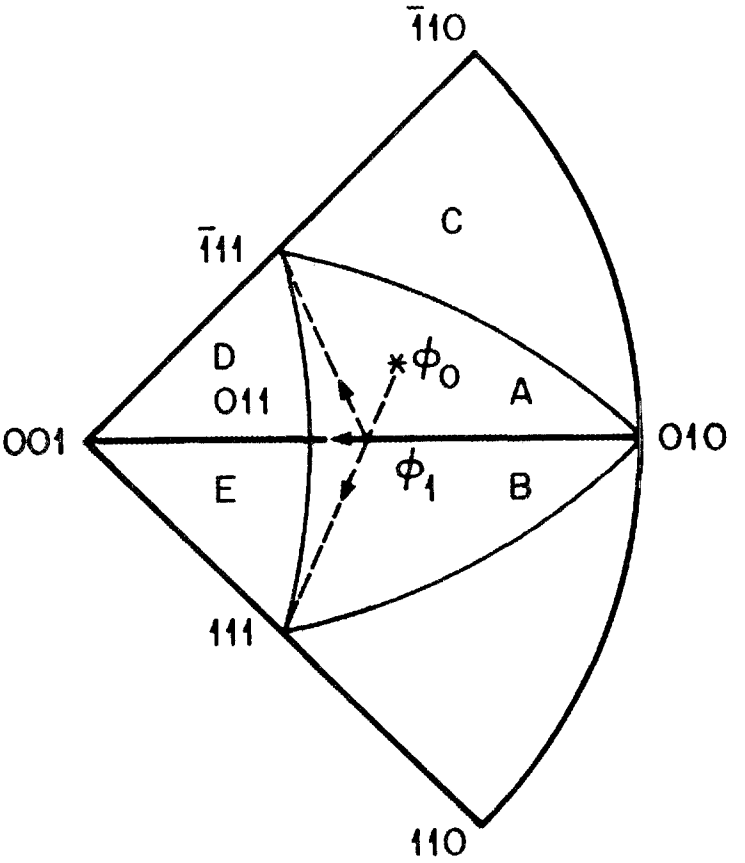

Fig. 6. Stereographic projection of TiAl illustrating the change in ϕ during compression.

a higher aluminum concentration than the matrix phase. Ordinary dislocations were observed near this particle (Figs. 13 and 14). The dislocations in Fig. 13 are of the [$\bar{1}$10] type. The dislocations marked ($\overline{mn}$) and ($\overline{pq}$) in Fig. 14 are of the a/2[110] type. Some stacking faults observed near this region were the only ones observed. Microprobe analysis indicates that the region near this inclusion has more titanium than the base Ti-56 at. % Al, indicating that the dislocation behavior may vary with the TiAl ratio in single-crystal samples. This needs further confirmation in single-crystal material.

ORNL-DWG 88-14102

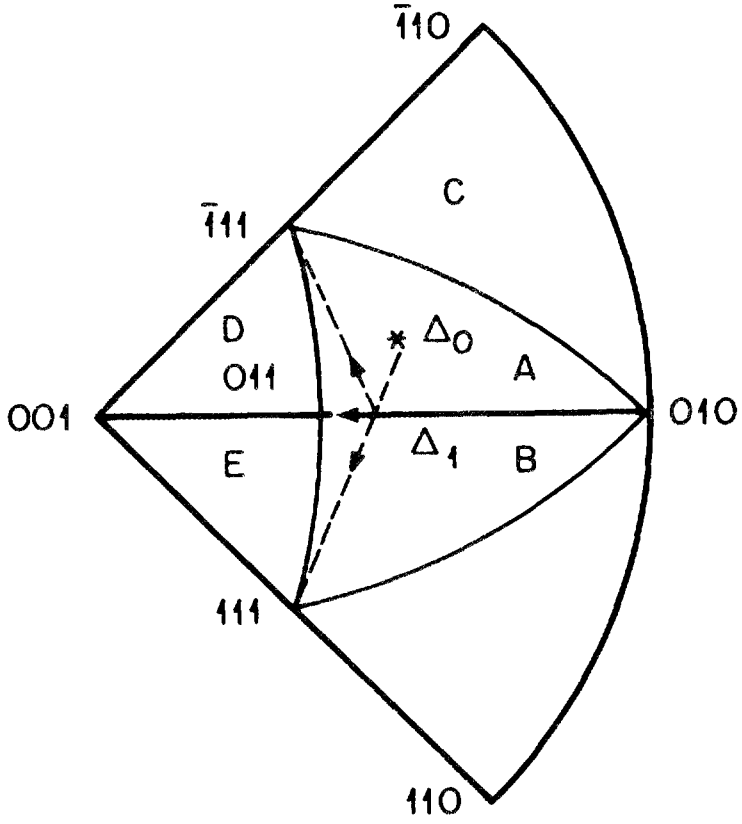

Fig. 7. Stereographic projection of TiAl illustrating the change in θ during compression.

ALLOY DEVELOPMENT

The initial intention of the alloy program was to identify promising alloys by arc-melting small melts and then examining both their single-crystal properties, utilizing the developed single-crystal process and equipment, and their polycrystalline single-phase properties. A good part of this program has been accomplished.

Despite the sophisticated processing developed in the first stage of this work, it is clear that high-aluminum-content, single-phase, binary TiAl alloys are very brittle. For this reason an alloy development program was undertaken to determine if ternary single-phase alloys could be

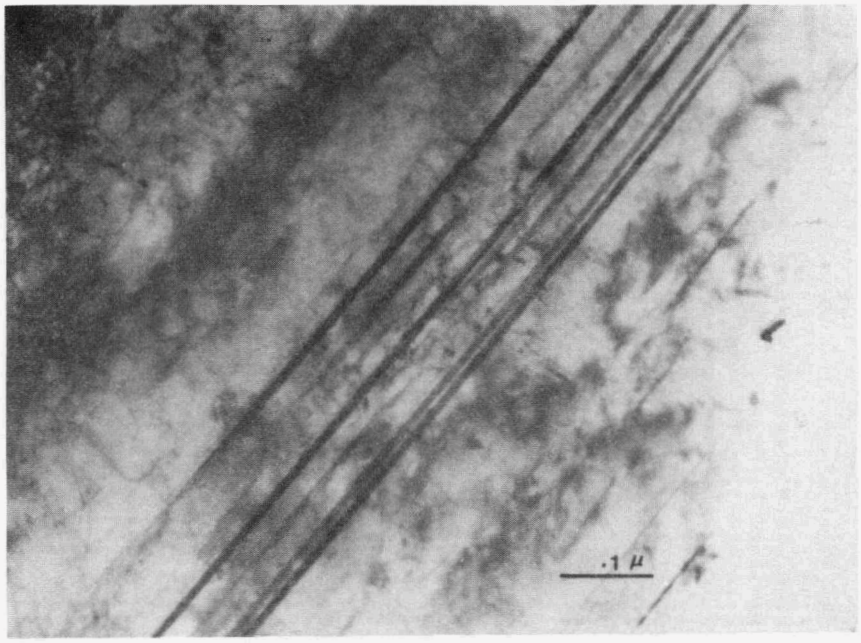

Fig. 8. Twin plates formed at a compressive load of 3.56×10^3 N. *Source:* University of Tennessee, Knoxville.

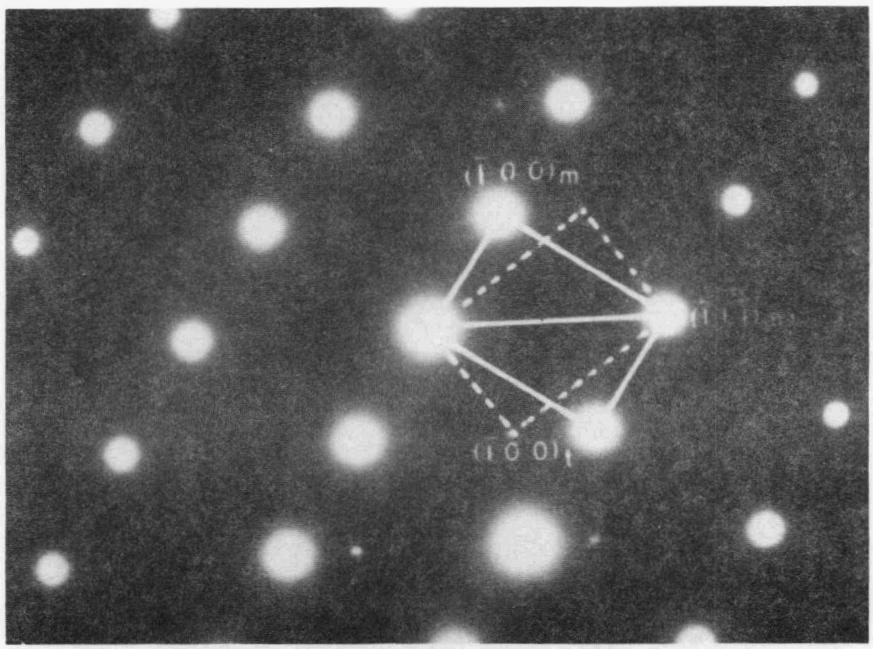

Fig. 9. Diffraction pattern of twins in Fig. 8. *Source:* University of Tennessee, Knoxville.

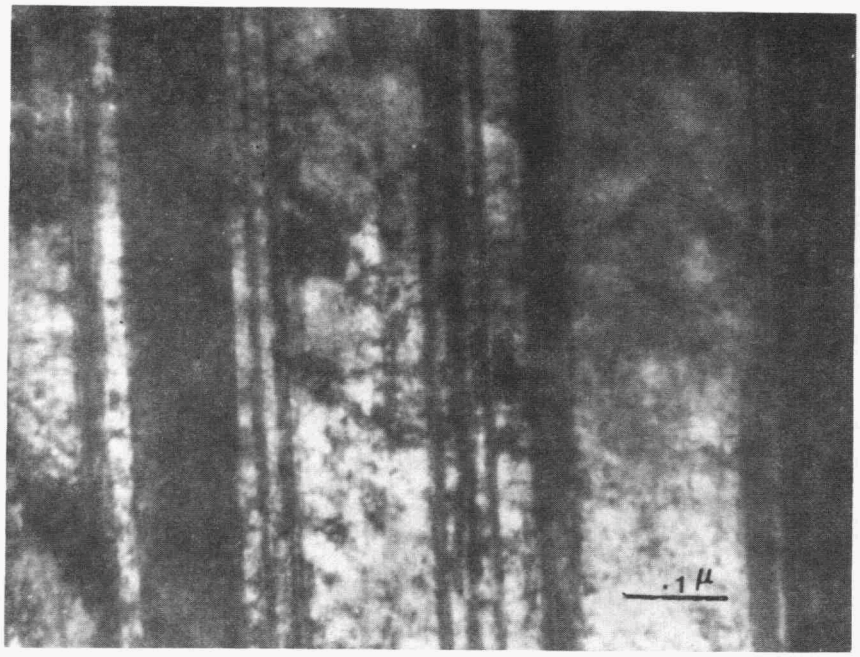

Fig. 10. Twins plates formed at a compressive strain of 0.5 and a load of 13.3×10^3 N. *Source:* University of Tennessee, Knoxville.

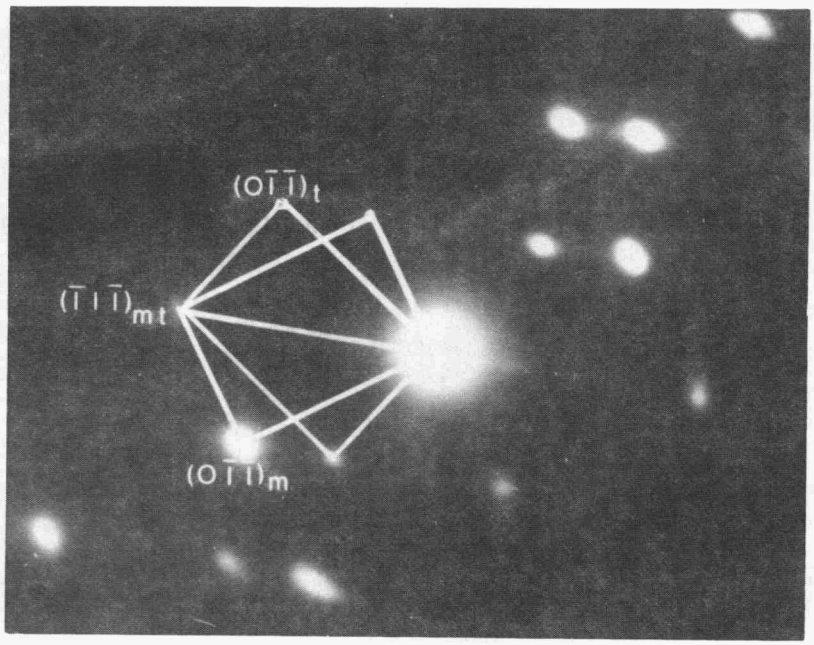

Fig. 11. Predominant twin plates of the $(1\bar{1}1)$ type. *Source:* University of Tennessee, Knoxville.

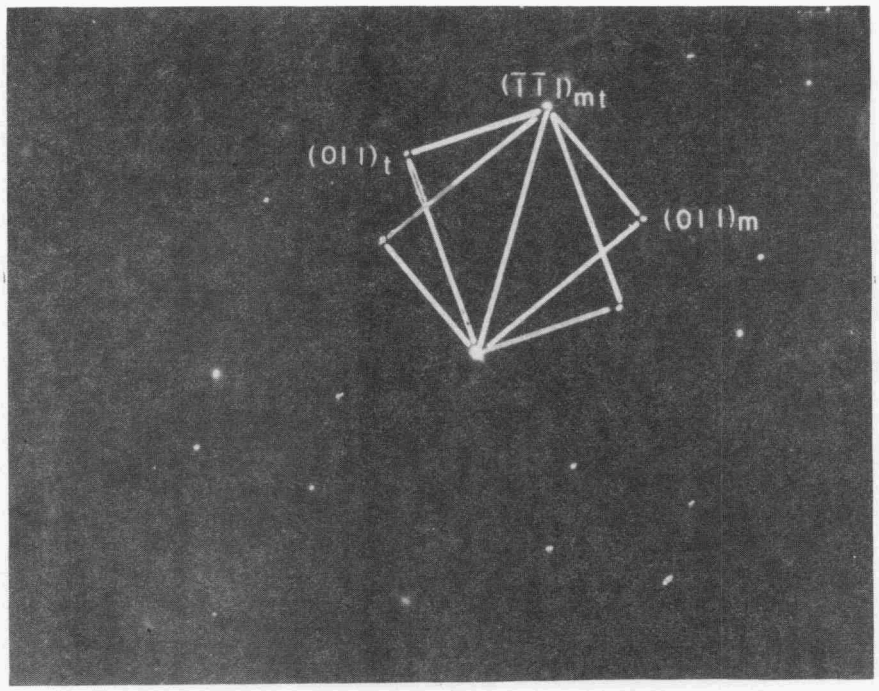

Fig. 12. Minor twins of the $(\bar{1}\bar{1}1)$ type.
Source: University of Tennessee, Knoxville.

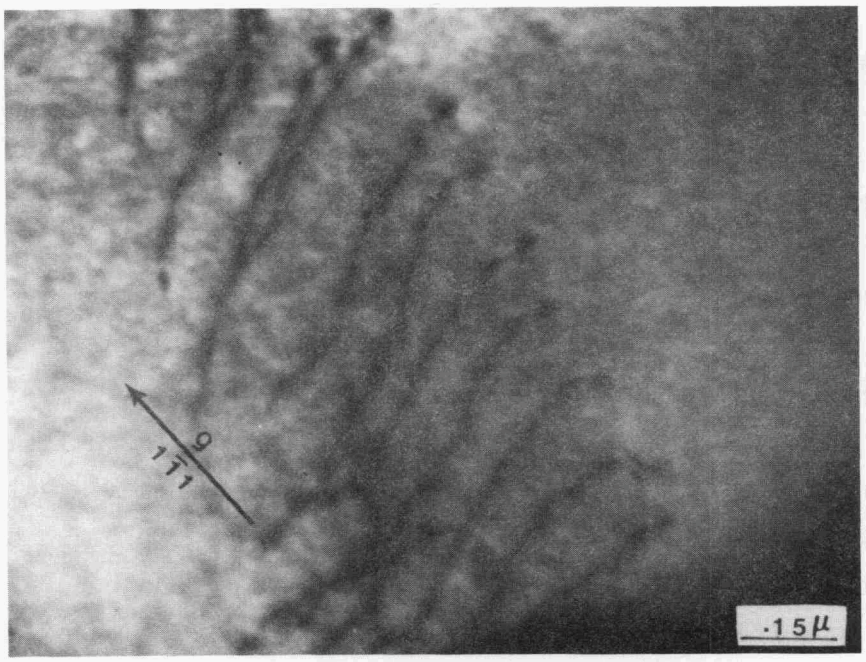

Fig. 13. $\langle\bar{1}10\rangle$ dislocations near inclusion.
Source: University of Tennessee, Knoxville.

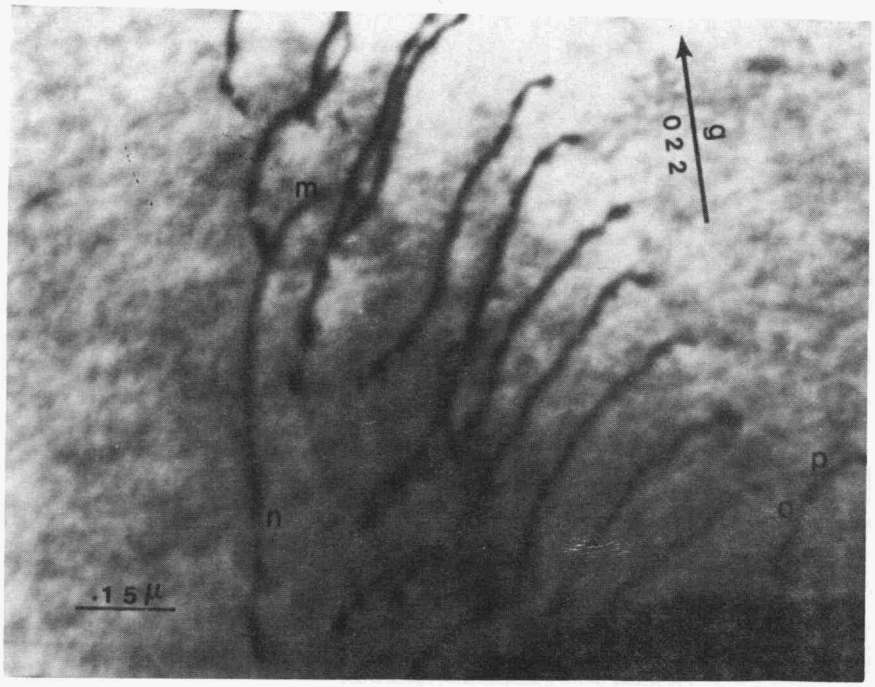

Fig. 14. $(\overline{mn})$, $(\overline{pq})$ dislocations of a/2[110] type. *Source:* University of Tennessee, Knoxville.

produced with higher room-temperature ductilities. The alloy program utilizes an arc melter to produce small, high-purity buttons of experimental heats. These were examined to show progress towards ductility development in TiAl. On the basis of structure map considerations, eight solutes were identified as showing promise within a "single-phase" constraint for the program. Of these eight, four were considered for experimental examination. Figure 15 shows the hardness of these single-phase alloys as a function of TiAl ratio.

The gallium alloy shows alloy softening (Fig. 15) with increasing Ti/Al ratios, especially at values greater than 1. This alloy also exhibits wavy slip in compression (Fig. 16) and grain boundary fracture in the cast structure (Fig. 17). This alloy shows excellent promise of further development. The manganese alloy, although harder than binary TiAl, is of interest for another reason. Figure 18 shows the as-cast and homogenized structure of a 5% manganese alloy. This alloy is slightly two-phase; however, the important feature of Fig. 18 is the large number of twins

ORNL-DWG 88-14103

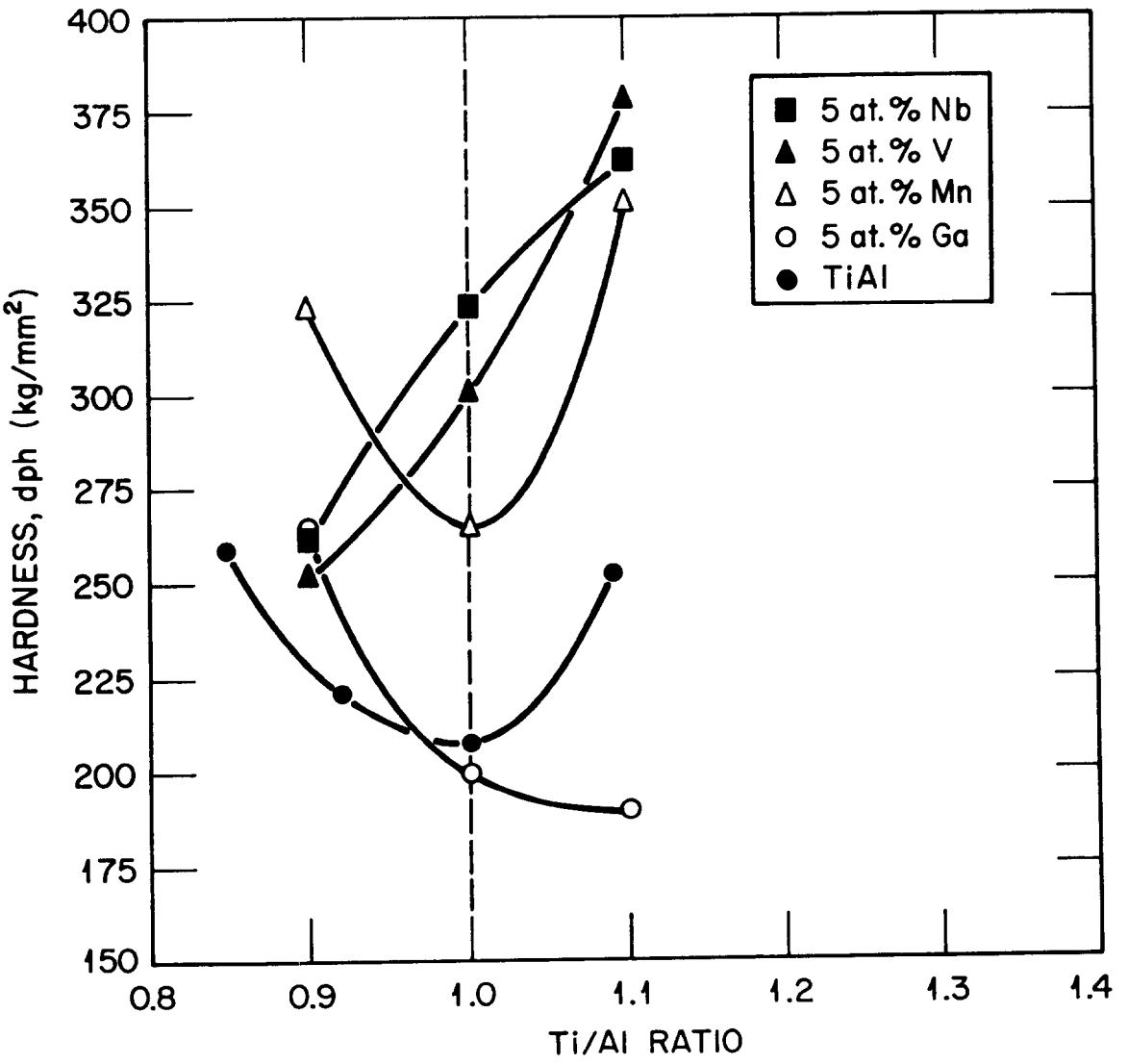

Fig. 15. Hardness as a function of Ti/Al for various ternary alloys.

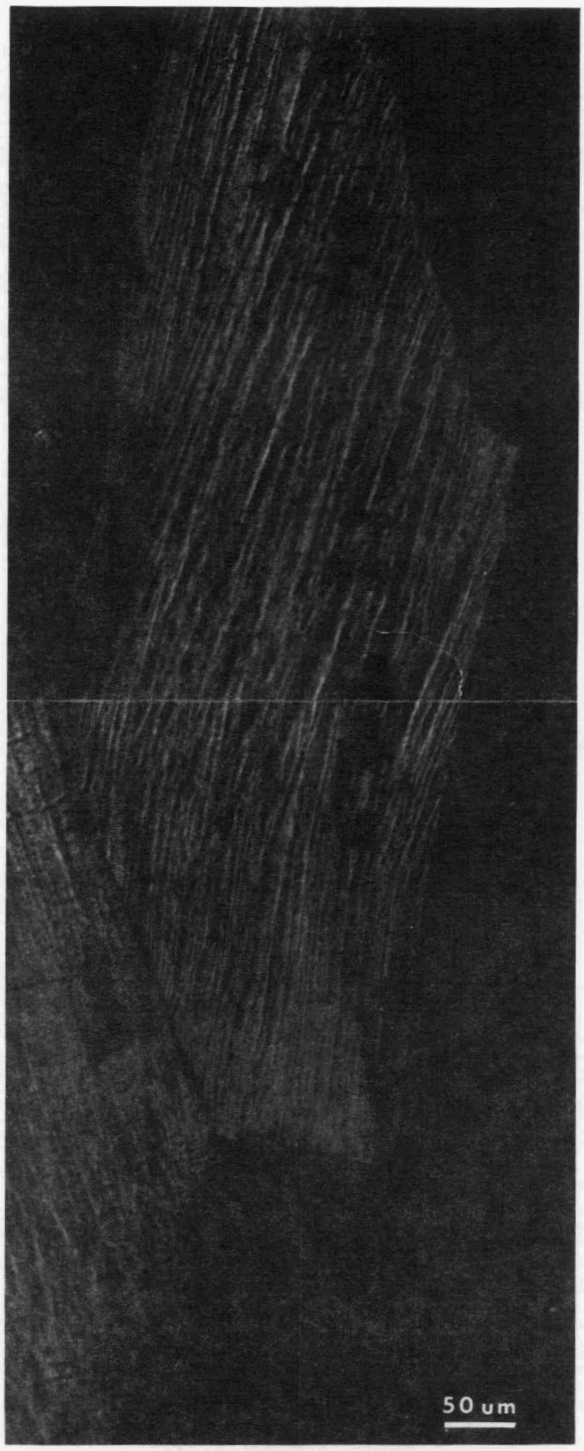

Fig. 16. Wavy slip in TiAl with gallium additions. *Source:* University of Tennessee, Knoxville.

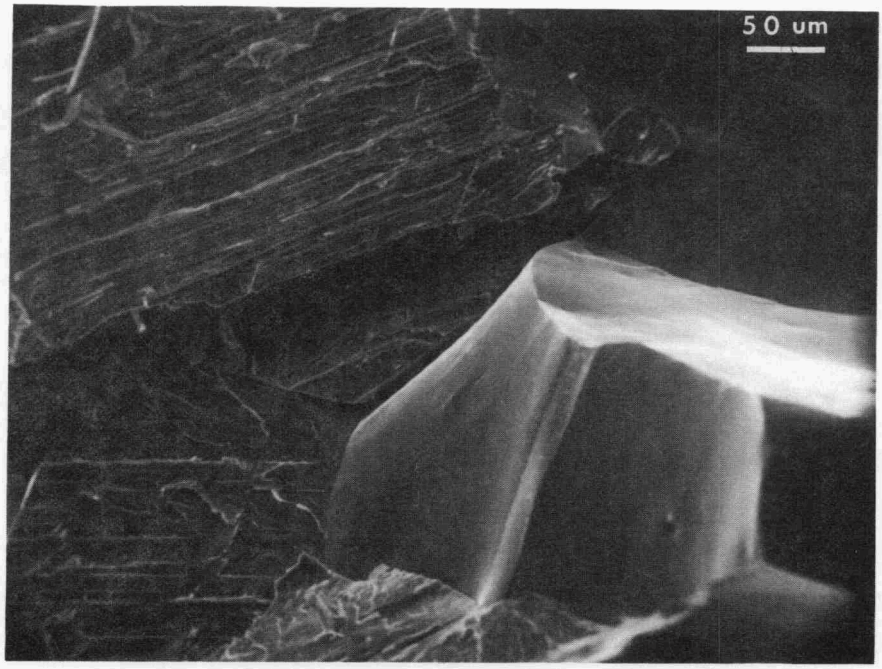

Fig. 17. Fracture surface of polycrystalline TiAl with gallium additions. *Source:* University of Tennessee, Knoxville.

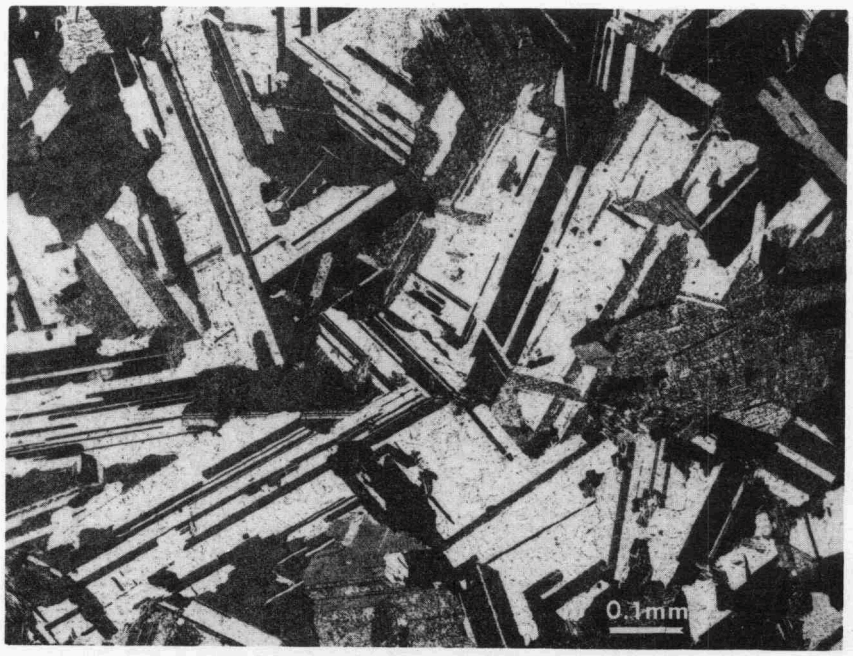

Fig. 18. Annealed structure of Ti/Al = 1.0 + 5 at. % Mn. Note annealing twins. *Source:* University of Tennessee, Knoxville.

present in the material. Clearly, the manganese additions have reduced the twin plane energy significantly. Figure 19 shows the same alloy after 5.9% compressive strain. The microtwins are evident. This twinning mechanism may improve the ductility of the alloy. Further work is required to determine if this is the case.

CONCLUSIONS

The following conclusions can be drawn from the present work:

1. Rapid growth in helium produces a substructure with about a 2° rotation in aluminum-rich TiAl.

2. Slower growth in helium results in samples with a large single-crystal core surrounded by surface grains of a rotated orientation with all grains growing off [011]. These crystals exhibit no substructure.

3. Slow growth (less than 2.5×10^{-2} m/h) in ultrapurity hydrogen can produce single crystals 2.54×10^{-2} m in diam by 0.1 m long without substructure or surface grains.

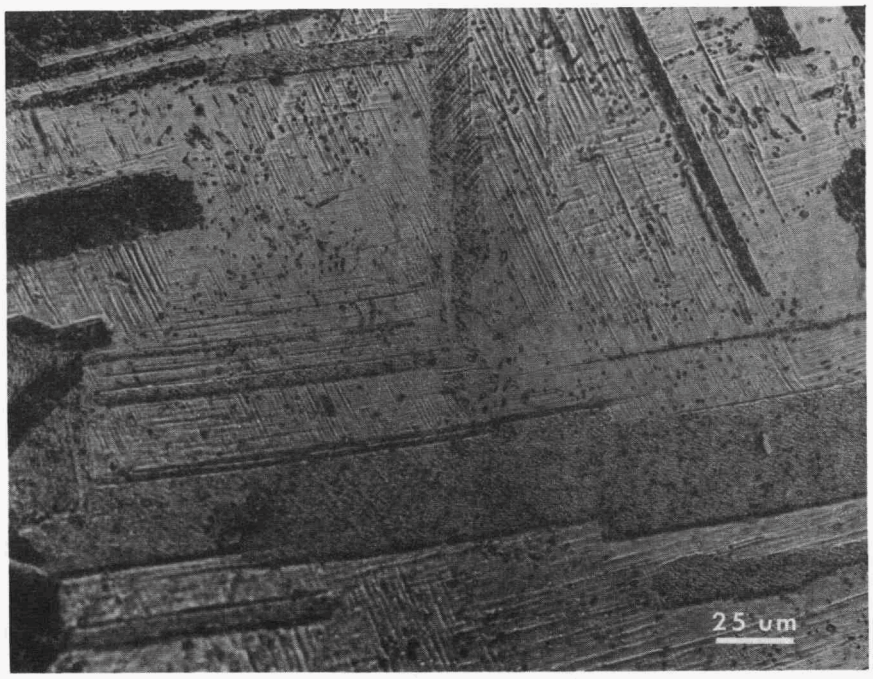

Fig. 19. Ti/Al = 1.0 + 5 at. % Mn. 59% compression. Note microtwinning. *Source:* University of Tennessee, Knoxville.

4. All crystals grown to date are off the [011] direction in orientation.

5. Significantly, TiAl may be processed in a hydrogen atmosphere without detrimental structural effects while possibly lowering interstitial contents.

6. Single crystal growth results from the strong anisotropy of crystal growth, allowing the competitive growth process to proceed under a stable computer control of growth parameters.

7. In single slip, stage I, low-density dislocation tangles develop.

8. Twinning plays an important role in the deformation of these alloys after a small initial plastic deformation by ordinary dislocation motion.

9. Twins have a $(\bar{1}\bar{1}1)$ axis. Their formation is not associated with the presence of stacking faults.

10. No superdislocations were observed in any of the samples except for several near an inclusion.

11. The observed dislocation behavior may vary with the Ti/Al ratio of the gamma phase.

12. Two alloys show promise for further development. One shows deformation by microtwinning and the other by wavy slip.

13. Hardness as a function of Ti/Al ratio and alloy content have been determined for additions of Nb, Mn, V, and Ga to TiAl.

REFERENCES

1. J. B. McAndrew and H. D. Kessler, "Ti-36% Al as a Base for High Temperature Alloys," *J. Met.* 8, 1348 (1956).

2. Robert E. Schafrik, "Dynamic Elastic Modulae of the Titanium Aluminides," *Met. Trans.* 8A, 1003 (1977).

3. C. C. Koch, C. T. Liu, and N. S. Stoloff, *High-Temperature Ordered Intermetallic Alloys*, 1st ed., Materials Research Society, Pittsburgh, 1984, p. 351.

4. P. L. Martin, M. G. Mendiratta, and H. A. Lipsitt, "Creep Deformation of Ti-Al and TiAl + W Alloys," *Met. Trans.* 14A, 2170 (1983).

5. Tokuzou Tsujimoto, Kenki Hashimoto, and Hiroo Suga, "Structures and Properties of an Intermetallic Compound: TiAl-Based Alloys Containing Silver," *Trans. Jpn Inst. Met.* 27, 341 (1986).

6. N. S. Stoloff, C. C. Koch, C. T. Liu, and O. Izumi, *High-Temperature Ordered Intermetallic Alloys*, 2nd ed., Materials Research Society, Pittsburgh, 1987, p. 481.

7. D. Shechtman, M. J. Blackburn, and H. A. Lipsitt, "The Plastic Deformation of TiAl," *Met. Trans.* 5, 1373 (1974).

8. H. A. Lipsitt, D. Shechtman, and R. E. Schafrik, "The Deformation and Fracture of TiAl at Elevated Temperatures," *Met. Trans.* 6A, 1991 (1975).

9. M. Gell, D. N. Duhl, D. K. Gupta, and K. D. Sheffler, "Advanced Superalloy Airfoils," *J. Met.* 11 (July 1987).

10. B. F. Oliver, "A Levitation-Zone Melter for Larger Diameter Bars with Positive Process Control," *Trans. AIME* 227, 960 (1963).

11. B. F. Oliver, "The Segregation of Tantalum in Iron in a Levitating-Zone Melter," *Trans. AIME* 230, 1352 (1964).

12. B. F. Oliver and F. Garofalo, "Immobilization of Interstitial Carbon During the Purification of Iron in a Zone-Melter," *Trans. AIME* 233, 1318 (1965).

13. B. F. Oliver, F. Garofalo, R. Priestner, and S. Arajs, *The Purification and Oxidation Zone Melting: Property Measurements and Minor Impurity Contents of Iron*, National Metallurgical Laboratory, Jamshedpur, India, Symposium Proceedings: Micro-Metallurgy (1964).

14. B. F. Oliver and E. W. Troy, "Oxidation-Zone Refining of Iron," *Mem. Sci. Rev. Metall.* 65 (June 1969).

15. A. J. Hatch, "Potential Well Description of Electromagnetic Levitation," *J. Appl. Phys.* 36(1) (Jan. 1965).

16. N. Fat-Halla, S. Bahi, T. Kawabata, and O. Izumi, "TiAl Single Crystals Obtained by the Floating Zone Technique," *Mater. Sci. Eng.* 61, 227 (1983).

17. T. Kawabata, T. Kanai, and O. Izumi, "Positive Temperature Dependence of the Yield Stress in TiAl $L1_0$ Type Superlattice Intermetallic Compound Single Crystals at 293–1273 K," *Acta Metall.* 33(7), 1355 (1985).

18. T. Kawabata and O. Izumi, "Dislocation Reactions and Fracture Mechanism in TiAl $L1_0$ Type Intermetallic Compound," *Scr. Metall.* **21**, 435 (1987).

19. R. Z. Schafrik, "Manufacture of TiAl by Extrusion of Blended Elemental Powders," *Met. Trans. B* 7B, 713 (1976).

20. G. Hug, A. Loiseau, and A. Lasalmonie, "Nature and Dissociation of the Dislocations in TiAl Deformed at Room Temperature," *Phil. Mag. A* 54, 45 (1986).

21. T. Kawabata and O. Izumi, "Dislocation Structures in TiAl Single Crystals Deformed at 77 K," *Scr. Metall.* **21**, 433 (1987).

22. B. F. Oliver, B. Y. Huang, and W. C. Oliver, "Containerless Growth of Large Single Crystals of TiAl," *Scr. Metall.* **22**(9), 1405-08 (1988).

23. R. L. Fleischer, "Single-Crystal Lattice Rotation During Compression," *J. Mech. Phys. Solids* 6, 301 (1958).

24. R. J. Price and A. Kelly, "Deformation of Age-Hardened Aluminum Alloy Crystal-1 Plastic Flow," *Acta Metall.* **12**, 159 (1964).

25. J. J. Hauser and K. A. Jackson, "Effect of Grip Constraints on the Tensile Deformation of F.C.C. Single Crystals," *Acta Metall.* **9**, 1 (1961).

26. R. L. Fleischer and B. Chalmers, "Grip Effects in the Deformation of Single Crystals," *J. Mech. Phys. Solids* 6, 307 (1958).

INTERNAL DISTRIBUTION

1-2. Central Research Library
3. Document Reference Section
4-5. Laboratory Records Department
6. Laboratory Records Department, RC
7. ORNL Patent Section
8-10. M&C Records Office
11. D. J. Alexander
12. P. Angelini
13. P. F. Becher
14. T. M. Besmann
15. R. A. Bradley
16. R. S. Carlsmith
17. R. H. Cooper, Jr.
18. D. F. Craig
19. S. A. David
20. E. P. George
21. F. M. Haggag
22. J. A. Horton, Jr.
23. E. A. Kenik
24. C. T. Liu
25. K. C. Liu
26. R. A. Lowden
27. C. G. McKamey
28-32. W. C. Oliver
33. W. D. Porter
34. A. C. Schaffhauser
35. T. M. Besmann
36. V. J. Tennery
37. J. R. Weir
38. F. W. Wiffen
39. M. H. Yoo
40. A. D. Brailsford (Consultant)
41. H. D. Brody (Consultant)
42. D. P. Pope (Consultant)
43. M. L. Savitz (Consultant)
44. E. R. Thompson (Consultant)
45. J. B. Wachtman (Consultant)

EXTERNAL DISTRIBUTION

46-48. AIR FORCE WRIGHT AERONAUTICAL LABORATORIES, Metals and Ceramics Division, Wright-Patterson Air Force Base, OH 45433

D. M. Dimiduk
Allan Katz
W. R. Kerr

49. ALUMINUM COMPANY OF AMERICA LABORATORIES, Alcoa Technical Center, Route 780, Seventh Street Road, Alcoa Center, PA 15269

G. MacZura

50. AMERICAN WELDING SOCIETY, 550 LeJeune Road, Miami, FL 33126

H. G. Ziegenfuss

51. BABCOCK & WILCOX COMPANY, 20 S. Van Buren Avenue, Barberton, OH 44203

J. E. Mack

52. CABOT CORPORATION, Technology Dept., 1020 W. Park Avenue, Kokomo, IN 46901

A. Asphahani

53. CARNEGIE-MELLON UNIVERSITY, Department of Metallurgical Engineering and Materials Science, Pittsburgh, PA 15213

T. B. Massalski

54. CASE WESTERN RESERVE UNIVERSITY, Department of Metallurgical and Materials Science, 10900 Euclid Ave., Cleveland, OH 44106

K. Vedula

55. CLIMAX MOLYBDENUM COMPANY, 1600 Huron Parkway, Ann Arbor, MI 48106

T. B. Cox

56. COMBUSTION ENGINEERING, INC., 911 W. Main Street, Chattanooga, TN 37401

D. A. Canonico

57-58. CORNELL UNIVERSITY, Ithaca, NY 14850

Che-Yu Li
S. L. Sass

59-60. CUMMINS ENGINE COMPANY, INC., Mail Code 50183, Box 3005, Columbus, IN 47202-3005

M. J. Patel
J. W. Patten

61-62. EG&G IDAHO, INC., Idaho National Engineering Laboratory, P.O. Box 1625, Idaho Falls, ID 83415

J. E. Flinn
R. N. Wright

63-66. ELECTRIC POWER RESEARCH INSTITUTE, 3412 Hillview Avenue, P.O. Box 10412, Palo Alto, CA 94303

W. T. Bakker
D. J. Frey
R. I. Jaffee
J. Stringer

67. EXXON RESEARCH AND ENGINEERING COMPANY, P.O Box 101, Florham Park, NJ 07932

G. Sorrell

68-69. GARRETT TURBINE ENGINE COMPANY, Advanced Materials, Materials Engineering, 111 South 34 Street, P.O. Box 5217, Phoenix, AZ 85010

G. S. Hoppin
B. Keiser

70. GA TECHNOLOGIES, P. O. Box 81608, San Diego, CA 92138

D. I. Roberts

71-73. GENERAL ELECTRIC COMPANY, Bldg. 81, Room E102, Schenectady, NY 12345

K. M. Chang
S. C. Huang
A. I. Taub

74. GENERAL ELECTRIC COMPANY, Corporate Research and Development, P.O. Box 8, Schenectady, NY 12301

R. L. Fleischer

75. GENERAL ELECTRIC COMPANY, Quartz and Chemicals Department, 24400 Highland Road, Richmond Heights, OH 44413

G. W. Weber

76. GENERAL ELECTRIC COMPANY, Mail Drop M89, Cincinnati, OH 45215

R. Darolia

77. INSTITUTE OF DEFENSE ANALYSES, 1801 Beauregard Street, Alexandria, VA 22311

T. F. Kearns

78. LEHIGH UNIVERSITY, Materials Research Center, Bethlehem, PA 18015

Y. T. Chou

79. LOCKHEED CORPORATION, Palo Alto Laboratories, 3251 Hanover Street, Palo Alto, CA 94303

E. C. Burke

80-82. LOS ALAMOS NATIONAL LABORATORY, Los Alamos, NM 87545

S. P. Chen
P. J. Hay
R. S. Skaggs

83-84. MICHIGAN TECHNOLOGICAL UNIVERSITY, Department of Metallurgical Engineering, Houghton, MI 49931

D. Mikkola
C. L. White

85. METALLAMICS, INC., P.O. Box 1539, Traverse City, MI 49684

R. R. McDonald

86. MONSANTO COMPANY, P.O. Box 1311, Texas City, TX 77590

P. S. Gupton

87. NAVAL SURFACE WEAPONS CENTER, Code R32, White Oak, Silver Spring, MD 20910

H. M. Dejarnette

88. NAVAL SURFACE WEAPONS CENTER, Surface Weapons Materials Technology Program, Dahlgren, VA 22448

W. T. Messick

89. NORTH CAROLINA A&T STATE UNIVERSITY, Department of Mechanical Engineering, Greensboro, NC 27411

V. S. Avva

90-91. NORTH CAROLINA STATE UNIVERSITY, Materials Engineering Dept., P.O. Box 7907, Raleigh, NC 27695

R. F. Davis
C. C. Koch

92. OAK RIDGE ASSOCIATED UNIVERSITIES LIBRARY, Oak Ridge, TN 37831

MERT Division

93. RENSSELAER POLYTECHNIC INSTITUTE, Materials Engineering Department, Troy, NY 12181

N. S. Stoloff

94. R. L. Smith, P.O. Box 98, Chassel, MI 49916

95. TENNESSEE TECHNOLOGY FOUNDATION, P.O. Box 23184, Knoxville, TN 37933

D. A. Patterson

96. TENNESSEE TECHNOLOGICAL UNIVERSITY, Center for Manufacturing Research and Technology Utilization, College of Engineering, Box 5014, Cookeville, TN 38505

J. T. Scardina

97. UNITED TECHNOLOGIES, Pratt and Whitney, Engineering Division, North, 400 Main Street, East Hartford, CT 06108

D. N. Duhl

98. UNIVERSAL CYCLOPS SPECIALTY STEEL DIVISION, 650 Washington Road, Pittsburgh, PA 15228

H. L. Black

99. UNIVERSAL ENERGY SYSTEMS, INC., 4401 Dayton-Xenia Road, Dayton, OH 45432

M. G. Mendiratta

100. UNIVERSITY OF CINCINNATI, Department of Materials Science and Engineering, Cincinnati, OH 45221-0012

J. A. Sekhar

101-111. UNIVERSITY OF TENNESSEE, Materials Science and Engineering Department, Knoxville, TN 37996

C. R. Brooks
B. Y. Huang (5)
B. F. Oliver (5)

112. UNIVERSITY OF TENNESSEE, Center for Materials Processing, College of Engineering, Knoxville, TN 37966-2000

J. C. Danko

113. VANDERBILT UNIVERSITY, Station B, P.O. Box 1621, Nashville, TN 37240

J. J. Wert

114. VIRGINIA POLYTECHNIC INSTITUTE AND STATE UNIVERSITY, Blacksburg, VA 24016

D. A. Farkas

115-117. DOE, ENERGY SYSTEMS RESEARCH AND DEVELOPMENT, Office of Conservation and Renewable Energy, Forrestal Building, Independence Avenue, Washington, DC 20585

J. J. Brogan
J. J. Eberhardt
S. M. Wolf

118. DOE, OAK RIDGE OPERATIONS, P.O. Box 2001, Oak Ridge, TN 37831-8600

Assistant Manager for Energy Research and Development

119-120. DOE, OFFICE OF SCIENTIFIC AND TECHNICAL INFORMATION, Office of Information Services, P.O. Box 62, Oak Ridge, TN 37831

For distribution by microfiche as shown in DOE/OSTI-4500, Distribution Category UC-365 (Energy Conservation)

☆U.S. GOVERNMENT PRINTING OFFICE 1990—748-114/20007